Design of Attitude and Rate Command Systems for Helicopters Using Eigenstructure Assignment

William L. Garrard,* Eicher Low,† and Scott Prouty‡
University of Minnesota, Minneapolis, Minnesota

This paper describes the use of eigenstructure assignment in the direct design of attitude and attitude rate command systems for helicopter flight control. Eigenvalue assignment is used to achieve desired bandwidth based on the handling qualities specifications, and eigenvector assignment is used to achieve decoupling of lateral, longitudinal, heave, and yaw modes and the desired command-response characteristics. Eigenstructure techniques are also used to design a state estimator that gives desired closed-loop frequency response. The stability robustness of the control system is evaluated with respect to an error model that includes rotor, actuator, flexure, and sensor dynamics and computational and sampling delays in the flight control system. The controlled helicopter is shown to exhibit both good frequency and time-response characteristics.

Nomenclature

Scalars

g	= acceleration of gravity
i	= $\sqrt{-1}$
m	= number of controls
n	= number of states
p	= roll rate, rad/s
q	= pitch rate, rad/s
r	= yaw rate, rad/s
s	= Laplace operator
u	= forward velocity, ft/s
u_1	= collective pitch, deg
u_2	= longitudinal cyclic pitch, deg
u_3	= lateral cyclic pitch, deg
u_4	= tail rotor collective pitch, deg
v	= lateral velocity, ft/s
w	= heave velocity, ft/s
X_q	= stability derivative associated with pitch rate
Y_p	= stability derivative associated with roll rate
z_i	= ith transmission zero
λ_i	= ith eigenvalue
$\underline{\sigma}(A)$	= minimum singular value of matrix A
$\bar{\sigma}(A)$	= maximum singular value of matrix A
θ	= pitch angle, rad
ϕ	= roll angle, rad

Vectors

$\boldsymbol{u}$	= control vector $[u_1, u_2, u_3, u_4]^T$
$\boldsymbol{v}_i$	= attainable closed-loop eigenvector associated

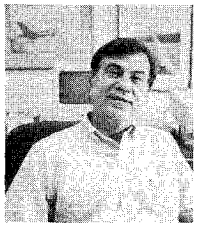

William L. Garrard, Professor and Associate Head of the Department of Aerospace Engineering and Mechanics at the University of Minnesota, received his B.S. in mechanical engineering and his Ph.D. in engineering mechanics from the University of Texas at Austin. Dr. Garrard's research interests include mathematical modeling and control of aircraft, helicopters and other aerospace vehicles, and parachute systems technology including mathematical modeling, wind-tunnel testing, structural analysis, and design. He has published and consulted extensively in all of these areas. Dr. Garrard has served on the AIAA Technical Committees on Guidance, Navigation, and Control, and Aerodynamic Deceleration and Balloon Technology. He is an Associate Fellow of AIAA and a member of IEEE and AHS.

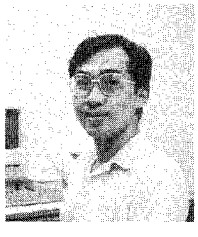

Eicher Low was born in Singapore in 1962. He received his B.S. degree in aeronautics and astronautics from the University of Washington in 1986 and an M.S. degree in aerospace engineering from the University of Minnesota in 1988. He is currently working on a Ph.D. degree in the Department of Aerospace Engineering and Mechanics. He is a member of AIAA and IEEE.

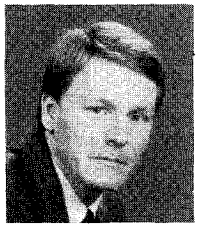

Born in Lime Ridge, Wisconsin, in 1962, Scott Prouty received his B.S. in mechanical engineering from the University of Wisconsin-Platteville in December 1985 and an M.S. in aerospace engineering from the University of Minnesota in December 1987. He is a student member of AIAA and is currently working for the Aerospace Corporation in El Segundo, California as a member of the technical staff in the Control Analysis Department.

Received Jan. 29, 1988; revision received May 8, 1988; presented as Paper 88-4141 at the AIAA Guidance, Navigation, and Control Conference, Minneapolis, MN, Aug. 15-17, 1988.

with λ_i eigenvalue
v_i^d = desired closed-loop eigenvector associated with λ_i eigenvalue
x_8 = state vector of rigid-body states $[u, v, w, p, q, r, \phi, \theta]^T$
$\hat{x}$ = estimate of rigid-body state vector
y = measurement vector $[w, p, q, r]^T$
μ_i = left zero direction of the ith finite transmission zero

Matrices

A = open-loop dynamics matrix
A^d = desired closed-loop dynamics matrix
B = control distribution matrix
B^d = desired control distribution matrix
C = measurement distribution matrix
$E(s)$ = multiplicative error matrix
$G_8(s)$ = open-loop transfer matrix, $C(Is - A)^{-1}B$
$F(s)$ = full-state loop transfer matrix, $K(Is - A)^{-1}B$
H = feedforward gain matrix
$K_8(s)$ = compensator transfer matrix, $K(Is - A + BK + LC)^{-1}L$
$K_8(s)G_8(s)$ = loop transfer matrix
K = feedback gain matrix
L = estimator gain matrix

Superscripts

d = desired
$*$ = complex transposed
T = transposed
-1 = inverse

Subscripts

c = commanded
8 = eighth-order model
32 = 32nd-order model

Introduction

THIS paper describes a methodology that uses eigenstructure assignment techniques for the design of helicopter flight control systems. The design of a flight control system for a four-bladed attack-type helicopter operating near hover is considered. The open-loop dynamics of this helicopter have deficiencies that are typical of most unaugmented, high-performance, single-rotor helicopters. These deficiencies are as follows: 1) there is substantial coupling between lateral and longitudinal modes, 2) both lateral and longitudinal responses are unstable, and 3) the bandwidths in the pitch, yaw, and heave axes are too low to satisfy level 1 handling qualities criteria.

Recent research in helicopter handling qualities indicates that, at low speeds or hover, pilots prefer rate or attitude command response in the roll, pitch, and yaw axes and velocity command in the heave direction.[1-4] Also at low speeds, decoupled longitudinal, lateral, yaw, and heave responses are desirable. This paper describes the use of eigenstructure assignment technique design flight control systems that yield properly decoupled closed-loop responses and give either attitude rate command or attitude command response in the pitch and roll axes, attitude rate command response in the yaw axis, and velocity command response in the heave direction. All of these responses exhibit specified frequency and time-response characteristics. Both feedback and feedforward control laws are synthesized, and an eigenstructure technique is used to design a state estimator in the feedback loop that gives desired closed-loop frequency-response characteristics.

Since rotor and other high-frequency dynamics can substantially limit helicopter flight control system bandwidth, it is necessary to include high-frequency dynamics in the design process.[5,6] In this paper, controller designs are developed using a model of the rigid-body dynamics that contains residualized advancing and regressing tip-path plane rotor modes.[7] Bandwidth limitations are established using an error model that contains rotor, actuator, and flexure dynamics; Padé approximations of digital computational and sampling delays; and a filter acting on the sensor outputs. Since the helicopter and flight control system constitutes a coupled, multivariable system, singular-value frequency-response techniques are used to determine stability bounds and allowable bandwidth. Time-history simulations illustrate the closed-loop response characteristics of the helicopter.

Mathematical Models

The mathematical model used for the design is typical of a modern attack helicopter operating near hover. The dynamics of the helicopter were originally modeled by a twelfth-order model that was composed of an eighth-order model representing the rigid-body dynamics and two second-order models representing the advancing and regressing rotor tip-path plane modes. Main rotor collective pitch, lateral cyclic pitch, longitudinal cyclic pitch, and tail rotor collective pitch were the control inputs.

An eighth-order design model that did not contain explicitly the tip-path plane modes was developed from the 12th-order model in order to simplify controller design and implementation. Since the tip-path plane modes were of considerably higher frequency than the rigid-body modes, the four states associated with these modes were eliminated from the design model by residualization.[7] As shown in Table 1, the eigenvalues of the residualized model are very close to those of the twelfth-order model.

The design model is written in state variable form as given next. The measured outputs are the pitch, roll, and yaw rates and heave velocity. The nondimensionalized A_8 and B_8 matrices are given in Table 2.

$$\dot{x}_8 = A_8 x_8 + B_8 u$$
$$y = C_8 x \tag{1}$$

Since the eigenvectors resulting from the dimensional state equations are also dimensional, the mixture of linear and angular dimensions made it difficult to identify the dominant modes associated with a particular eigenvalue. Consequently, the state and control vectors were nondimensionalized so that modal couplings could be more easily identified. The state vector was nondimensionalized by dividing all the linear velocity components by 16.67 ft/s (10 knots), all the angular velocities by 0.349 rad/s (20 deg/s), and all the angular displacements by 0.349 (20 deg). These are the nominal variations in forward velocity, attitude angles, and angular rates for which the linearized hover model is considered accurate. The control inputs were nondimensionalized by dividing by their maximum values. These were 9 deg for collective pitch, 8.75 deg for lateral cyclic pitch, 15 deg for longitudinal cyclic pitch, and 18.5 deg for tail rotor collective pitch.

The open-loop eigenvalues and nondimensional eigenvectors for the residualized hover model are given in Table 3. As can be seen from these values, there is considerable coupling among all modes. Roll rate is coupled to yaw rate. Side slip is coupled to yaw rate, pitch rate, and forward velocity. Forward velocity is coupled to yaw rate, roll rate, and side slip. Pitch rate is coupled to yaw rate, and yaw and heave are heavily coupled. The eigenvalues associated with the side slip and forward velocity are unstable with rapid doubling times. Also, the bandwidth in the pitch rate, yaw rate, and heave modes is too low for level 1 handling qualities.[1-4]

The eighth-order design model described previously gives a reasonably accurate representation of the helicopter dynamics for frequencies up to approximately 10 rad/s; however, studies have shown that high-frequency effects such as rotor dynam-

Table 1 Eigenvalues for twelfth- and eighth-order models

$A_8 =$

−0.0199	−0.0058	−0.0058	−0.0151	0.0232	0.0006	0.0000	−0.6652
−0.0452	−0.0526	−0.0061	−0.0260	−0.0155	0.0148	0.6648	−0.0003
−0.0788	−0.0747	−0.3803	0.0008	−0.0048	0.0420	0.0228	0.0102
0.4557	−2.5943	−0.1787	−2.9979	−0.5308	0.4155	0.0000	0.0000
0.3688	0.1931	−0.1753	0.0710	−0.5943	0.0013	0.0000	0.0000
1.0939	0.7310	−0.0358	0.4058	0.4069	−0.4940	0.0000	0.0000
0.0000	0.0000	0.0000	1.0000	0.0005	−0.0154	0.0000	0.0000
0.0000	0.0000	0.0000	0.0000	0.9994	0.0343	0.0000	0.0000

$B_8 =$

−0.0456	−0.0083	0.4735	−0.0016
−0.0369	0.2785	0.0086	0.3600
−3.1126	−0.0032	0.0076	0.0002
−2.4241	20.8327	1.0196	9.1903
−0.3205	0.2538	−6.3329	−0.0648
5.7889	−2.6208	2.3832	−11.0904
0.0000	0.0000	0.0000	0.0000
0.0000	0.0000	0.0000	0.0000

Table 2 Nondimensional A and B matrices for eighth-order model

Twelfth-order model		Eighth-order residualized model
$-4.3434 + 0.0000i$		$-3.2377 + 0.0000i$ Roll rate
$0.2130 + 0.5270i$		$0.2110 + 0.5296i$ Forward velocity
$0.0328 + 0.7499i$		$0.0353 + 0.7431i$ Side slip
$-0.9421 + 0.0000i$		$-0.9021 + 0.0000i$ Pitch rate
$-0.5654 + 0.0000i$		$-0.5695 + 0.0000i$ Yaw rate
$-0.3234 + 0.0000i$		$-0.3221 + 0.0000i$ Heave velocity
$-13.6446 + 72.1554i$	Advancing rotor mode	
$-11.7698 + 3.6620i$	Regressing rotor mode	

Table 3 Open-loop eigenvalues and associated nondimensional eigenvectors

	Roll rate	Side slip	Forward velocity
	$\lambda = -3.2377 + 0.0000i$	$\lambda = 0.0353 \pm 0.7431i$	$\lambda = 0.2110 \pm 0.5296i$
u	$0.0071 + 0.0000i$	$0.1239 \pm 0.0691i$	$0.1078 \mp 0.4243i$
v	$0.0692 + 0.0000i$	$-0.1740 \pm 0.5037i$	$-0.1781 \pm 0.1191i$
w	$0.0063 + 0.0000i$	$-0.0429 \mp 0.0285i$	$-0.0023 \pm 0.0273i$
p	$0.9407 + 0.0000i$	$0.0898 \mp 0.4337i$	$-0.1138 \pm 0.0301i$
q	$-0.0308 + 0.0000i$	$0.0936 \pm 0.0437i$	$-0.0952 \mp 0.1698i$
r	$-0.1557 + 0.0000i$	$0.3095 \pm 0.1069i$	$-0.4358 \mp 0.5712i$
ϕ	$-0.2913 + 0.0000i$	$-0.5791 \mp 0.1419i$	$0.0433 \pm 0.2102i$
θ	$0.0112 + 0.0000i$	$0.0703 \mp 0.1368i$	$-0.3800 \pm 0.0565i$
	Pitch rate	Yaw rate/heave velocity	
	$\lambda = -0.9021 + 0.0000i$	$\lambda = -0.5695 + 0.0000i$	$\lambda = -0.3221 + 0.0000i$
u	$0.3787 + 0.0000i$	$-0.1589 + 0.0000i$	$-0.0858 + 0.0000i$
v	$0.0364 + 0.0000i$	$0.0710 + 0.0000i$	$-0.1097 + 0.0000i$
w	$0.1027 + 0.0000i$	$-0.2290 + 0.0000i$	$-0.3863 + 0.0000i$
p	$0.0031 + 0.0000i$	$0.0633 + 0.0000i$	$-0.0317 + 0.0000i$
q	$-0.4160 + 0.0000i$	$0.0413 + 0.0000i$	$0.0419 + 0.0000i$
r	$-0.6597 + 0.0000i$	$0.9421 + 0.0000i$	$-0.9080 + 0.0000i$
ϕ	$-0.0145 + 0.0000i$	$-0.0857 + 0.0000i$	$0.0550 + 0.0000i$
θ	$0.4860 + 0.0000i$	$-0.1291 + 0.0000i$	$-0.0332 + 0.0000i$

ics, airframe flexibility, actuator and sensor dynamics, and so forth, can cause instabilities when high bandwidth feedback controllers are synthesized.[5,6] It is impossible to accurately model all important high-frequency dynamics and other uncertainties. Furthermore, a design model that contains high-frequency dynamics will result in high-order feedback compensators that are difficult to implement. Consequently, the approach taken in this study is to develop an error model that provides an estimate of the worst-case modeling uncertainties and then to develop a compensator design that guarantees stability based on their error model. The error model was developed from the study of a 32nd-order model that consisted of 1) the eight rigid-body states; 2) the four tip-path plane states; 3) first-order models of the four control actuators; 4) second-order models of the airframe flexure dynamics in pitch, roll, yaw, and heave; 5) a first-order Padé approximation of digital time delays; and 6) a first-order filter on the sensor outputs. A block diagram of the system on which the 32nd-order model is based is shown in Fig. 1.

The actuators were represented as first-order with break frequencies of 60 rad/s. The flexure dynamics were idealized as second-order with damping ratios of 0.05 and natural frequencies of 35 rad/s for heave, 50 rad/s for pitch and roll rate, and 30 rad/s for yaw rate. The first-order Padé filter approxi-

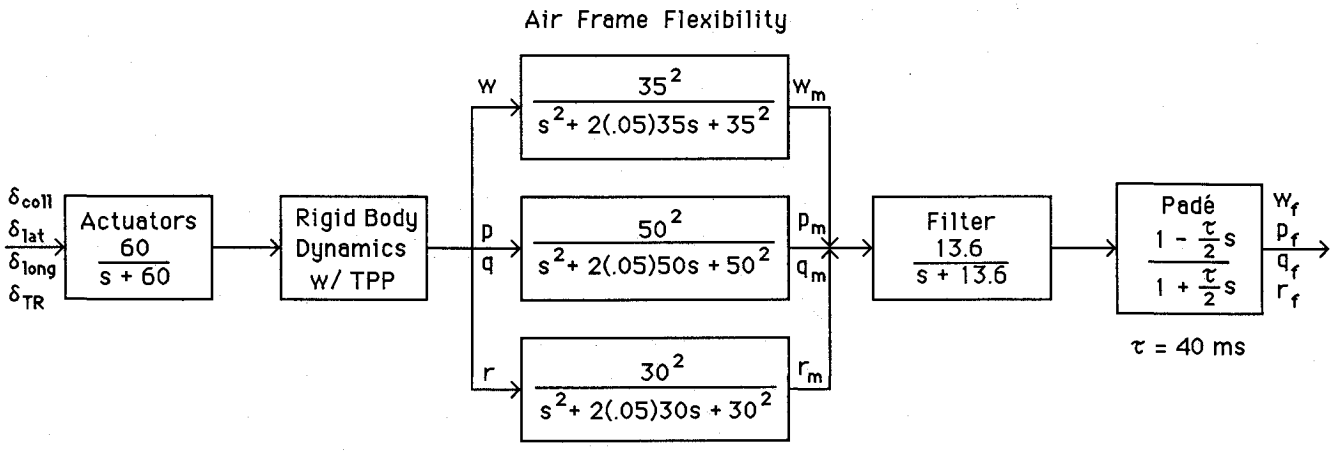

Fig. 1 Block diagram for 32nd-order model.

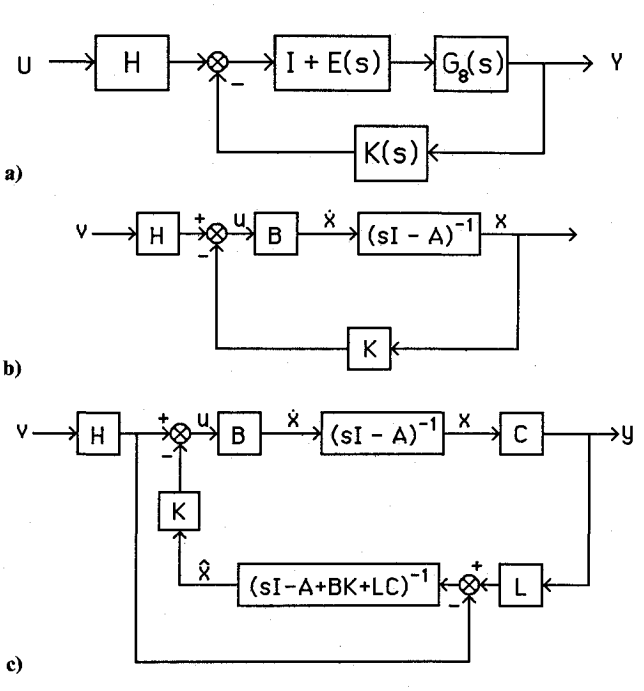

Fig. 2 Block diagrams for various feedback configurations. a) Feedback system with multiplicative error matrix. b) Full-state feedback. c) Estimator in feedback loop.

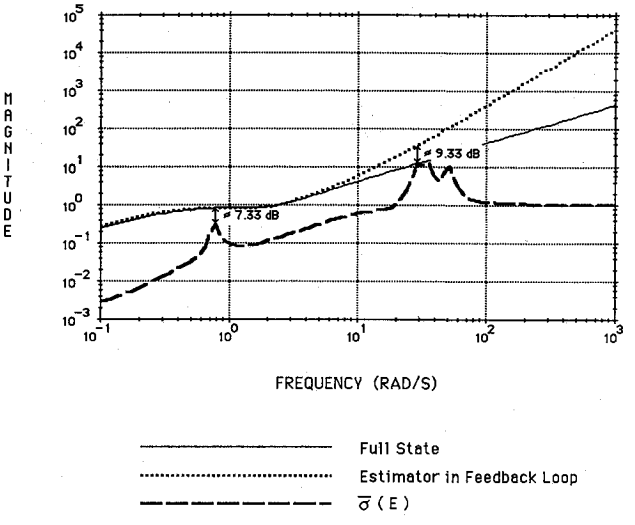

Fig. 3 Stability robustness for closed-loop systems. Full-state and estimator in feedback loop.

mates the time delay of the digital computer with τ equal to 40 ms. A first-order filter for attenuation of 4/rev rotor vibrations was also included in this model. The rotor speed was 34 rad/s; therefore, the break frequency of the filter was selected as 13.6 rad/s, 10% of the 4/rev frequency.

The transfer matrix between the control inputs and outputs for the design model is obtained from Eq. (2) as

$$G_8(s) = C_8(sI - A_8)^{-1}B_8 \tag{2}$$

With Fig. 1, a multiplicative (relative) error model was developed.[8] The "true" transfer matrix was considered to be that given by a higher-order model selected to give a worst-case error bound. The true and design transfer matrices are related by

$$G_{true}(s) = G_8(s)[I + E(s)] \tag{3}$$

Since $G_{true}(s)$ and $G_8(s)$ are known, the error can be calculated as

$$E(s) = G_8^{-1}(s)G_{true}(s) - I \tag{4}$$

It should be emphasized that $G_{true}(s)$ is simply our best estimate of the relationship between the inputs and outputs from which a worst-case error bound can be deduced.

A block diagram of the closed-loop system with the multiplicative error is given in Fig. 2a. $K_8(s)$ represents the compensator transfer matrix. A sufficient condition for stability is

$$\underline{\sigma}\{I + [K_8(s)G_8(s)^{-1}\} > \bar{\sigma}[E(s)] \qquad \text{for} \qquad s = j\omega \tag{5}$$

where $0 < \omega < \infty$.[8-10]

A worst-case error bound was generated by removing portions of the 32nd-order model and seeing what effect this had on the maximum singular value of $E(s)$. If the true model is assumed to consist only of the rigid-body and tip-path plane states, the error is small. This is to be expected since the design model is based on residualization of a model containing the tip-path plane modes. Inclusion of the actuators results in only a small increase in error compared with the rigid-body, tip-path plane model. Inclusion of the flexure modes results in a substantial increase in the error. The error increases still further when the true model is comprised of only the rigid-body, tip-path plane, and flexure modes. Addition of the Padé approximation and sensor filter reduces the error. Inclusion of actuators, sensor filters, and Padé approximations attenuated the effect of the flexure modes and the model that gave the worst-case error was 20th-order and contained only rigid-body, tip-path plane, and flexure modes. Since it is well known that it is difficult to accurately model

the dynamics of helicopters by linearized perturbation models, it was decided to use a worst-case error estimate for evaluation of stability robustness. Figure 3 shows the error decreasing for frequencies greater than about 50 rad/s. In fact, this is not correct because of the presence of unmodeled higher-frequency modes. Large relative modeling errors cannot be avoided as frequency increases. Based on this reasoning, the modeling error is estimated to lie within the region shown in Fig. 3. If the modeling error is indeed within this region, stability is assured if Eq. (5) is satisfied.

Use of Eigenstructure Assignment for Direct Design of Attitude Response and Attitude Rate-Response Systems

For many tasks, helicopter pilots appear to desire either attitude rate or attitude rate response about both the pitch and roll axes.[1-4] In attitude response systems, the desired transfer function between commanded and actual roll angle is second-order

$$\phi/\phi_c = \omega_{n\phi}^2/(s^2 + 2\xi_\phi\omega_{n\phi}s + \omega_{n\phi}^2) \tag{6}$$

In a roll attitude rate-response system, the desired transfer function between commanded and actual rates is

$$p/p_c = (\tau_\phi s + 1)\omega_{n\phi}^2/(s^2 + 2\xi_\phi\omega_{n\phi}s + \omega_{n\phi}^2) \tag{7}$$

Similar frequency-response characteristics are desired about the pitch axis. The desired yaw rate and heave velocity transfer functions are first-order and are given by

$$r/r_c = \lambda_r/(s + \lambda_r) \tag{8}$$

$$w/w_c = \lambda_w/(s + \lambda_w) \tag{9}$$

The values of ξ, ω_n, λ, and τ are determined from handling qualities criteria. Level 1 handling qualities appear to result for bandwidths greater than 2 rad/s. For second-order attitude command systems of the type given in Eq. (6), bandwidth is defined as the frequency at which the phase angle of the transfer function between command input and output is -135 deg.[1,2,4] This bandwidth is related to the natural frequency and damping factor by

$$\omega_{bw} = \omega_n[\zeta + (\zeta^2 + 1)^{1/2}] \tag{10}$$

As long as the damping is reasonably large, the flying qualities are relatively insensitive to the damping factor.[1,2] For first-order systems, the bandwidth was taken to be the break frequency. Since modal decoupling is required, the open-loop transfer matrix between the commanded inputs and outputs, $G_8(s)$, should be diagonal with the diagonal elements given by either Eqs. (6) or (7), (8), and (9).

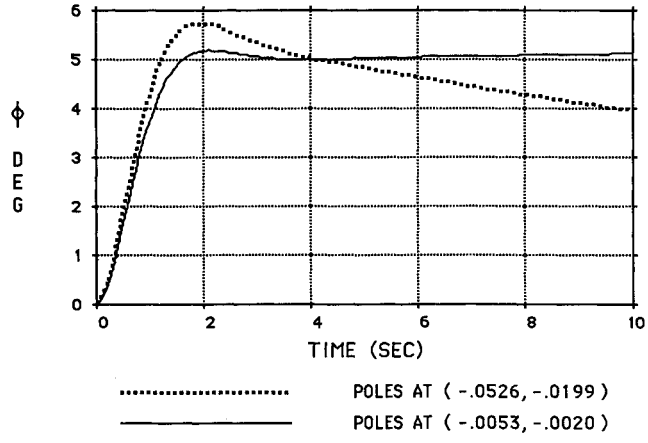

Fig. 4 Comparison of time response for roll command for two closed-loop low-frequency pole locations.

Eigenstructure assignment techniques are time domain procedures, whereas handling quality specifications are given mostly in the frequency domain. Eigenstructure assignment can be used to design controllers that satisfy these specifications by defining a state-space model of the closed-loop system that yields the desired frequency-response characteristics and modal decoupling. This model is then used to define the desired eigenvalue/eigenvector configurations that are to be achieved by eigenstructure assignment (the details of eigenstructure assignment are given in Refs. 11–14).

The desired closed-loop state equations for the helicopter are as given in Eq. (11).

$$\dot{x} = A^d x + B^d x_c \tag{11}$$

where

$$A^d = \begin{bmatrix} -\lambda_u & 0 & 0 & 0 & X_q & 0 & 0 & -g \\ 0 & -\lambda_v & 0 & Y_p & 0 & 0 & g & 0 \\ 0 & 0 & -\lambda_w & 0 & 0 & 0 & 0 & 0 \\ 0 & 0 & 0 & -2\zeta\omega_{n\phi} & 0 & 0 & -\omega_{n\phi}^2 & 0 \\ 0 & 0 & 0 & 0 & -2\zeta\omega_{n\theta} & 0 & 0 & -\omega_{n\theta}^2 \\ 0 & 0 & 0 & 0 & 0 & -\lambda_r & 0 & 0 \\ 0 & 0 & 0 & 1 & 0 & 0 & 0 & 0 \\ 0 & 0 & 0 & 0 & 1 & 0 & 0 & 0 \end{bmatrix}$$

$$B^d = \begin{bmatrix} 0 & 0 & 0 & 0 \\ 0 & 0 & 0 & 0 \\ \lambda_w & 0 & 0 & 0 \\ 0 & \omega_{n\phi}^2 & 0 & 0 \\ 0 & 0 & \omega_{n\theta}^2 & 0 \\ 0 & 0 & 0 & \lambda_r \\ 0 & 0 & 0 & 0 \\ 0 & 0 & 0 & 0 \end{bmatrix}$$

Examination of Eq. (11) reveals that the lateral, longitudinal heave and yaw modes are decoupled. In addition, forward velocity is decoupled from the pitch equation and side velocity from the roll equation. The resulting transfer functions be-

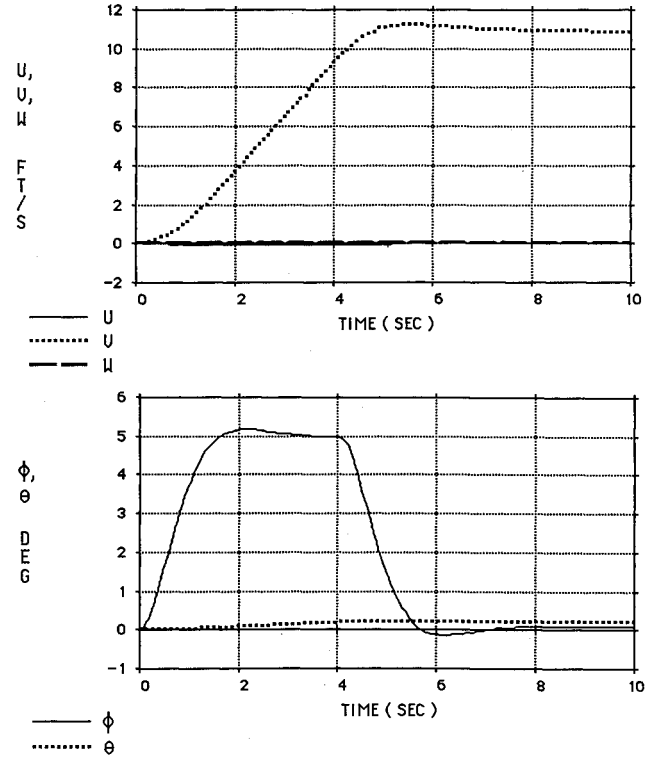

Fig. 5 Full-state closed-loop response to a 5 deg roll command of 4 s duration.

tween the commanded inputs and outputs are as given in Eqs. (6–9). Attitude rate command response can be obtained by prefiltering the roll and pitch inputs by $(\tau s + 1)/s$.

In Eq. (11), the natural coupling of pitch and pitch rate into the forward velocity equation and roll and roll rate into the side velocity equation is maintained. The resulting transfer function between side velocity and roll command is

$$\frac{v(s)}{\phi_c(s)} = \frac{\omega_{n\phi}^2(-Y_p s + g)}{(s - \lambda_v)(s^2 + 2\zeta\omega_{n\phi}s + \omega_{n\phi}^2)} \tag{12}$$

The eigenvalues $-\lambda_u$ and $-\lambda_v$ are associated with the linearized drag forces in the forward and side directions.

Six of the closed-loop desired eigenvalues were selected to give bandwidths of 4 rad/s about the pitch and roll axes, a bandwidth of 2 rad/s about the yaw axis, and a bandwidth of 2 rad/s in the heave direction. A damping factor of 0.707 was chosen for the complex poles. The closed-loop desired eigenvalues for forward velocity and side slip, $-\lambda_u$ and $-\lambda_v$, respectively, were initially left at their nominal values of -0.0199 and -0.0526; however, it was found that values of -0.00199 and -0.00526 improved steady-state response about the roll and pitch axes. By using the foregoing set of eigenvalues, the desired closed-loop eigenvectors were generated from Eq. (12). The desired and achievable closed-loop eigenvalues and eigenvectors and the required full-state feedback gain matrix are given in Tables 4 and 5.

Even though the resulting gain matrix achieved excellent modal decoupling for initial condition errors, response to control inputs was unsatisfactory because of extensive coupling in the control distribution matrix B. A matrix of feedforward gains was designed to alleviate this problem. The desired control distribution matrix B^d is given in Eq. (12). The feedforward gain matrix H was selected such that

$$B * H \approx B^d \tag{13}$$

Since B is nonsquare, it is necessary to solve for H using the optimal pseudoinverse

$$H = (B^T B)^{-1} B^T * B^d \tag{14}$$

The block diagram of the full-state controller with the feedforward gains is shown in Fig. 2b.

Time-history responses were calculated with the eigenvalues associated with the side and forward velocity modes initially located at -0.0526 and -0.0119, respectively. Examination of these responses revealed that for times of up to about 4 s, the responses were as desired; however, as time increased, the steady-state values of the roll angle decreased from the desired value (see Fig. 4). Since only the long period (low-frequency) response was not as desired, the low-frequency eigenvalues associated with side forward velocity and side slip were decreased by a factor of 10 to -0.00526 and -0.00199. As shown in Fig. 4, this improved both transient and steady-state response. Handling qualities requirements specify only that these velocity responses be stable. The full-state design passed the stability robustness condition given in Eq. (6) (see Fig. 3).

The degree of decoupling achieved in the closed-loop system is demonstrated by the response to a roll axis command of 5 deg that is held for 4 s and then returned to zero (see Fig. 5). All velocities are plotted on the same graph to the same scale, as are the angular positions. Roll angle is second-order and pitch angle is negligible as are forward and heave velocities. A roll command also results in an acceleration command/velocity hold type of response in the side velocity.[15] Once the roll attitude achieves its commanded value, the side or forward acceleration remains essentially linear until the roll command returns to zero. The roll attitude then returns to zero and the velocity remains essentially constant. There is some decay of velocity, but it is small because the eigenvalues associated with the forward and side velocity were selected to be small. The responses to a pitch angle command were similar to the responses to a roll angle command. First-order decoupled heave velocity and yaw rate commands were also achieved.

The frequency-response characteristics of the transfer functions between the commanded and actual roll angle are shown in Fig. 6. This plot shows second-order response with bandwidths of 4 rad/s. The pitch axis transfer function was essentially the same as that for the roll axis. The heave velocity and yaw rate transfer functions were first-order with bandwidths of 2 rad/s.

State Estimator Design

The full-state regulator described previously requires that all states be fed back. Since only heave, pitch rate, roll rate, and yaw rate are measured, it is necessary to include a state estimator in the feedback loop in order to implement the control law. The control is given by

$$\boldsymbol{u} = -K\hat{\boldsymbol{x}} \tag{15}$$

Table 4 Desired eigenstructure

	Side velocity	Roll	Pitch
	$\lambda = -0.00526$	$\lambda = -1.5000 + 1.5000i$	$\lambda = -1.4500 + 1.4500i$
u	$0.0000 + 0.0000i$	$0.0000 + 0.0000i$	$-0.0996 + 0.1095i$
v	$1.0000 + 0.0000i$	$-0.1403 + 0.0075i$	$-0.0000 + 0.0000i$
w	$0.0000 + 0.0000i$	$0.0000 + 0.0000i$	$0.0000 + 0.0000i$
p	$0.0000 + 0.0000i$	$0.0000 + 0.8956i$	$0.0000 + 0.0000i$
q	$0.0000 + 0.0000i$	$0.0000 + 0.0000i$	$-0.6286 - 0.6286i$
r	$0.0000 + 0.0000i$	$0.0000 + 0.0000i$	$0.0000 + 0.0000i$
ϕ	$0.0000 + 0.0000i$	$0.2985 - 0.2985i$	$0.0000 + 0.0000i$
θ	$0.0000 + 0.0000i$	$0.0000 + 0.0000i$	$0.0000 + 0.4335i$
	Forward velocity	Yaw rate	Heave velocity
	$\lambda = -0.00199$	$\lambda = -2.0000$	$\lambda = -2.1000$
u	$1.0000 + 0.0000i$	$0.0000 + 0.0000i$	$0.0000 + 0.0000i$
v	$0.0000 + 0.0000i$	$0.0000 + 0.0000i$	$0.0000 + 0.0000i$
w	$0.0000 + 0.0000i$	$0.0000 + 0.0000i$	$1.0000 + 0.0000i$
p	$0.0000 + 0.0000i$	$0.0000 + 0.0000i$	$0.0000 + 0.0000i$
q	$0.0000 + 0.0000i$	$0.0000 + 0.0000i$	$0.0000 + 0.0000i$
r	$0.0000 + 0.0000i$	$1.0000 + 0.0000i$	$0.0000 + 0.0000i$
ϕ	$0.0000 + 0.0000i$	$0.0000 + 0.0000i$	$0.0000 + 0.0000i$
θ	$0.0000 + 0.0000i$	$0.0000 + 0.0000i$	$0.0000 + 0.0000i$

Table 5 Achievable closed-loop eigenstructure and nondimensional full-state gains

	Achievable eigenstructure		
	Side velocity	Roll	Pitch
	$\lambda = -0.00526$	$\lambda = -1.5000 \pm 1.5000i$	$\lambda = -1.4500 \pm 1.4500i$
u	$0.0008 + 0.0000i$	$-0.0018 \pm 0.0035i$	$-0.0534 \pm 0.1363i$
v	$0.9977 + 0.0000i$	$-0.1285 \pm 0.0044i$	$0.0039 \pm 0.0036i$
w	$0.0022 + 0.0000i$	$0.0004 \mp 0.0000i$	$-0.0013 \mp 0.0004i$
p	$0.0034 + 0.0000i$	$0.0003 \pm 0.8970i$	$-0.0006 \pm 0.0005i$
q	$-0.0009 + 0.0000i$	$0.0004 \pm 0.0004i$	$-0.6238 \pm 0.6337i$
r	$-0.0003 + 0.0000i$	$0.0003 \mp 0.0001i$	$0.0001 \mp 0.0002i$
ϕ	$-0.0649 + 0.0000i$	$0.2989 \mp 0.2991i$	$0.0004 \pm 0.0003i$
θ	$0.0169 + 0.0000i$	$0.0000 \mp 0.0003i$	$-0.0034 \pm 0.4334i$
	Forward velocity	Yaw rate	Heave velocity
	$\lambda = -0.00199$	$\lambda = -2.0000$	$\lambda = -2.1000$
u	$0.9985 + 0.0000i$	$-0.0027 + 0.0000i$	$0.0275 + 0.0000i$
v	$-0.0001 + 0.0000i$	$-0.0254 + 0.0000i$	$-0.0285 + 0.0000i$
w	$-0.0005 + 0.0000i$	$-0.0006 + 0.0000i$	$0.9992 + 0.0000i$
p	$-0.0007 + 0.0000i$	$0.0065 + 0.0000i$	$0.0035 + 0.0000i$
q	$-0.0008 + 0.0000i$	$-0.0075 + 0.0000i$	$0.0046 + 0.0000i$
r	$0.0000 + 0.0000i$	$0.9995 + 0.0000i$	$-0.0007 + 0.0000i$
ϕ	$0.0360 + 0.0000i$	$0.0044 + 0.0000i$	$-0.0017 + 0.0000i$
θ	$0.0417 + 0.0000i$	$-0.0134 + 0.0000i$	$-0.0022 + 0.0000i$

Nondimensional full-state feedback gain matrix

$$K = \begin{bmatrix} 0.0243 & 0.0242 & -0.5524 & -0.0002 & 0.0008 & -0.0136 & -0.0073 & -0.0046 \\ 0.0686 & -0.1072 & 0.499 & 0.0193 & 0.0483 & 0.0901 & 0.2389 & 0.1105 \\ -0.0459 & -0.0245 & 0.0597 & -0.0085 & -0.3616 & -0.0040 & 0.0154 & -0.6622 \\ -0.1120 & -0.0332 & -0.2841 & -0.0431 & -0.1254 & -0.1650 & -0.0569 & -0.1708 \end{bmatrix}$$

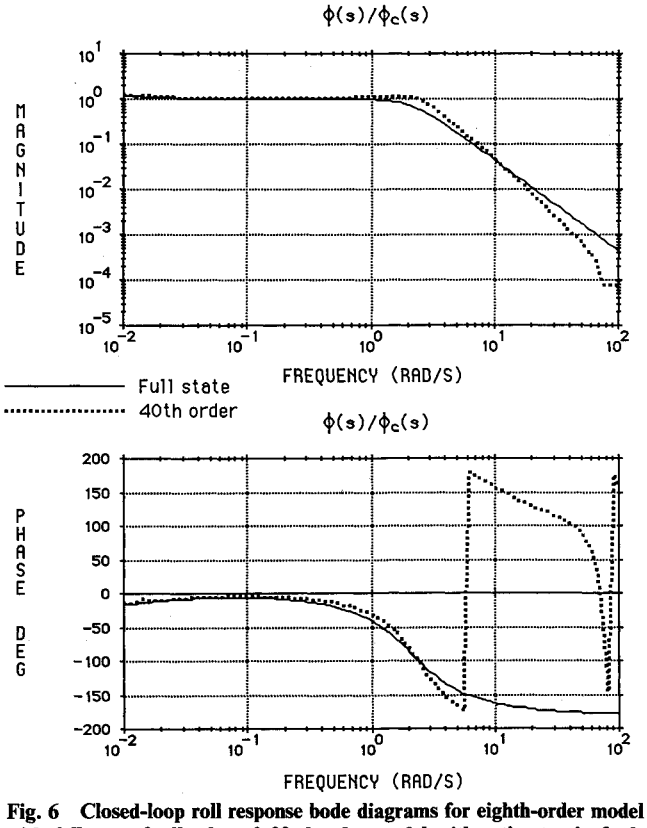

Fig. 6 Closed-loop roll response bode diagrams for eighth-order model with full-state feedback and 32nd-order model with estimator in feedback loop.

where $\hat{x}$ is the estimate of the state given by the state estimator

$$\dot{\hat{x}} = A_8\hat{x} + B_8u + L(y - C_8\hat{x}) \tag{16}$$

The block diagram of the system with the estimator in the feedback loop is given in Fig. 2c. The task is to choose the estimator gain matrix L, such that $A - LC$ is stable and the frequency response of the system with the regulator/estimator in the feedback loop closely resembles that for full-state feedback. That is,

$$K_8(s)G_8(s) \approx F(s) \tag{17}$$

This is called loop transfer recovery (LTR). The procedure using eigenstructure assignment algorithms for the design of estimators that achieve LTR is as follows[16]:

1) Determine the finite transmission zeros z_i and associated left zero directions of the open-loop system μ_i.

2) Drive the j finite eigenvalues of $A - LC$ to (or near) the finite transmission zeros z_i. The associated desired left eigenvectors should be chosen as μ_i.

3) Place the remaining $n - j$ eigenvalues of $A - LC$ at locations "far" into the left-half plane. These are called infinite eigenvalues. The desired left eigenvectors for these modes are chosen arbitrarily and have little effect on the LTR.

Improved LTR is obtained as the finite eigenvalues are moved closer to the transmission zeros and as the infinite eigenvalues are moved farther left. On the other hand, as the infinite eigenvalues are moved farther left, the estimator bandwidth is increased.

The four finite open-loop transmission zeros of the helicopter are

$$z_{1,2} = 0.0$$

$$z_{3,4} = -0.000734 \pm 0.01398i$$

The four desired eigenvalues and eigenvectors of the estimator were placed at the four transmission zero positions and their respective left zero directions. The values of z_1 and z_2 were approximated by -0.001 and 0.0015 because of computational difficulties arising from multiple roots. The remaining four closed-loop eigenvalues were placed at -10.0 rad/s and

Table 6 Nondimensional estimator gain matrix

Nondimensional estimator gain matrix L			
0.2309	−0.0057	−0.7419	0.0282
−0.4086	+0.0710	0.0201	−0.2572
9.6208	0.0118	0.0117	0.0439
−0.0632	6.9775	−0.5740	0.4876
−0.1743	0.0733	9.3784	−0.0029
−0.0393	0.4140	0.3254	9.4891
−0.0002	1.0000	0.0013	−0.0153
−0.0002	−0.001	1.0011	0.0339

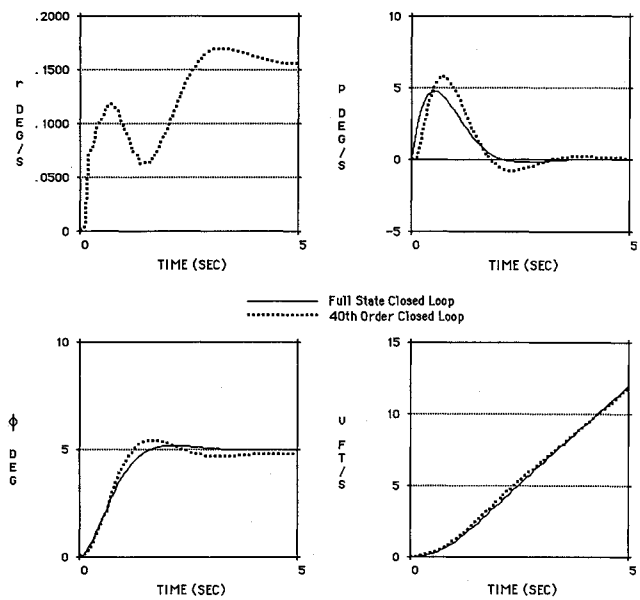

Fig. 7 Closed-loop lateral responses to a 5 deg roll command for eighth-order model with full-state feedback and 32nd-order model with estimator in feedback loop.

their corresponding eigenvectors were arbitrarily chosen. As shown in Fig. 3, this configuration achieves full LTR up to 7 rad/s. Above this frequency, the presence of the estimator in the feedback loop results in an additional 20 dB/decade of rolloff, thereby enhancing robustness compared with the full-state regulator. A measure of the robustness of a multi-input/multi-output (MIMO) system is the minimum difference between the minimum singular value of $[I + (KG_8)^{-1}]$ and the maximum singular value of the multiplicative error $E(s)$. This can be regarded as an MIMO gain margin. As shown in Fig. 3, the minimum differences between the two curves are 7.33 dB at about 0.8 rad/s and 9.33 dB at 30 rad/s.

The nondimensional estimator gain matrix is given in Table 6. The resulting feedback gains are of reasonable magnitude for actual implementation. The excessively large gains and concomitant high bandwidths that were obtained in a previous eigenstructure design for a similar helicopter were avoided by appropriate placement of the infinite eigenvalues.[17] Lower estimator gains were required to obtain recovery when the infinite eigenvalues were placed on the negative real axis rather than in a Butterworth pattern. These gains were further reduced by placing all the infinite eigenvalues at the same location on the negative real axis. It is important to place the infinite eigenvalues no farther to the left than is required to achieve LTR necessary for stability robustness. As the infinite eigenvalues are placed farther to the left, the estimator bandwidth is increased and sensor noise may become a problem.

Performance Evaluation

The time response of the helicopter was evaluated using the 32nd-order helicopter model with the estimator in the feedback loop resulting in a 40th-order simulation model. Simulations of the time response for a 5 deg step command in roll for the 40th-order model including the estimator in the feedback loop and the 8th-order model using the full-state controller are compared in Figs. 7 and 8. It can be seen that the responses are very similar. The roll angle and roll rate responses are second-order in both cases. The damping is slightly less for the 40th-order system model; however, damping is still heavy enough to result in good handling qualities as measured by current criteria.[1-4] Side velocity response is essentially indistinguishable between the two models. The heave, pitch, and yaw responses are small in magnitude in both the eight- and 40th-order models; thus, these responses are plotted to a larger scale and the differences are more apparent. The effects of the high-frequency dynamics in the 40th-order model can be seen in the initial transient responses. Similar results were obtained for the heave, pitch, and yaw inputs.

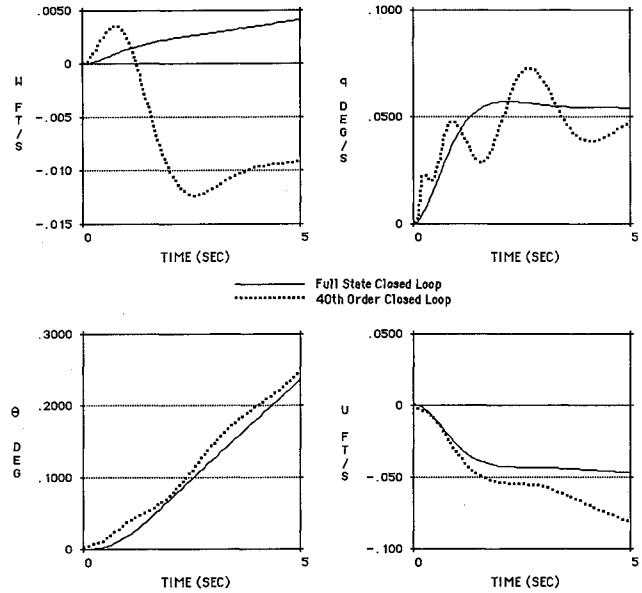

Fig. 8 Closed-loop longitudinal responses to a 5 deg roll command for eighth-order model with full-state feedback and 32nd-order model with estimator in feedback loop.

Bode plots between roll command and actual roll angle for the 40th-order model are shown in Fig. 6. Based on the eighth and 40th-order models, the magnitudes do not diverge significantly until about 50 rad/s and the phase angles are about the same until 6 rad/s (Fig. 6). If the pilot is regarded as a pure gain and the roll attitude loop is closed by the pilot, the gain margin in this channel is about 20 dB. Similar results are obtained for the pitch transfer function, except the gain margin is about 10 dB. The magnitudes of the heave velocity transfer functions based on the eighth- and 40th-order models are identical to a frequency of about 30 rad/s; however, the phase difference between the two transfer functions becomes apparent at about 2 rad/s. The gain margin in this channel is about 14 dB. The yaw rate transfer functions are very similar to the heave velocity transfer functions. In all cases, the frequency-response characteristics of the 40th-order model are very close to those of the eighth-order model in the frequency range in which pilot commands are anticipated.

Conclusions

Eigenstructure assignment appears to provide a useful and straightforward methodology for the design of helicopter flight control systems that provide for 1) modal decoupling, 2) desired command-response characteristics, and 3) good stability robustness. In addition, the estimator design achieves good loop transfer recovery without high gains and excessive bandwidth.

Acknowledgment

This research was supported by the Army Research Office under Contract DAAL03-86-K-0056.

References

[1]Hoh, R. H., Mitchell, D. G., Ashkanas, I. L., Aponso, B. L., Ferguson, S. W., and Rosenthal, T. J., "Proposed Airworthiness Design Standard: Handling Qualities Requirements for Military Rotorcraft," System Technology, Inc., Hawthorne, CA, TR 1194-2, Dec. 1985.

[2]Mitchell, D. G., Hoh, R. H., Morgan, J. M., "A Flight Investigation of Helicopter Low-Speed Response Requirements," *Proceedings of the AIAA Atmospheric Flight Mechanics Conference*, AIAA, New York, 1987, pp. 1–11.

[3]Lewis, M. S., Mansur N. H., and Chen, R. T. N., "A Simulator Investigation of Parameters Affecting Helicopter Handling Qualities in Air to Air Combat," *Proceedings 43rd Annual Forum*, American Helicopter Society, Alexandria, VA, 1987, pp. 645–662.

[4]Mitchell, D. G. and Hoh, R. H., "Development of Time Response Criteria for Rotorcraft at Hover and Low Speeds," *Proceedings of the AIAA, 12th Atmospheric Flight Mechanics Conference*, AIAA, New York, 1985.

[5]Chen, R. T. N. and Hindson, W. S., "Influence of High-Order Dynamics on Helicopter Flight-Control System Bandwidth," *Journal of Guidance, Control, and Dynamics*, Vol. 9, March–April 1986, pp. 190–197.

[6]Hall, W. E., Jr. and Bryson, A. E., "Inclusion of Rotor Dynamics in Controller Design," *Journal of Aircraft*, Vol. 10, April 1973, pp. 200–206.

[7]Hansen, R. S., "On Approximating Higher-Order Rotor Dynamics in Helicopter Stability-Derivative Models," AIAA Paper 83-2088, Aug. 1983.

[8]Doyle, J. C. and Stein, G., "Multivariable Feedback Design: Concepts for a Classical/Modern Synthesis," *IEEE Transactions on Automatic Control*, Vol. 26, Feb. 1981, pp. 4–16.

[9]Stein, G. and Athans, M., "The LQG/LTR Procedure for Multivariable Feedback Control Design," *IEEE Transactions on Automatic Control*, Vol. 32, Feb. 1987, pp. 105–115.

[10]Lehtomaki, N. A., Sandell, N. R., and Athans, M., "Robustness Results in Linear Quadratic Based Multivariable Controller Design," *IEEE Transactions on Automatic Control*, Vol. 26, Feb. 1981, pp. 75–92.

[11]Garrard, W. L. and Liebst, B. S., "Active Flutter Suppression Using Eigenspace and Linear Quadratic Design Techniques," *Journal of Guidance, Control, and Dynamics*, Vol. 8, May–June 1985, pp. 304–311.

[12]Liebst, B. S., Garrard, W. L., and Adams, W. M., "Design of an Active Flutter Suppression System," *Journal of Guidance, Control, and Dynamics*, Vol. 8, Jan.–Feb. 1986, pp. 64–71.

[13]Moore, B. C., "On the Flexibility Offered by Full State Feedback In Multivariable Systems Beyond Closed Loop Eigenvalue Assignment," *IEEE Transactions on Automatic Control*, Vol. 21, Oct. 1976, pp. 682–691.

[14]Andry, A. N., Shapiro, E. Y., and Chung, J. C., "On Eigenstructure Assignment for Linear Systems," *IEEE Transactions on Aerospace Systems*, Vol. AES-19, Sept. 1983, pp. 711–729.

[15]Mitchell, D. G., Hoh, R. H., and Atencio, A., "Classification of Response-Types for Single Pilot NOE Helicopter Response Tasks," *Proceedings of the 43rd Annual Forum*, American Helicopter Society, Alexandria, VA, 1987, pp. 663–676.

[16]Kazerooni, H. and Houpt, P. K., "On the Loop Transfer Recovery," *International Journal of Control*, Vol. 43, No. 3, 1986, pp. 981–996.

[17]Garrard, W. L. and Liebst, B. S., "Design of a Multivariable Flight Control System for Handling Qualities Enhancement," *Proceedings of the 43rd Annual Forum*, American Helicopter Society, Alexandria, VA, 1987, pp. 677–696.